



This information is current as of December 1, 2017.

## Innate Immune Activation by cGMP-AMP Nanoparticles Leads to Potent and Long-Acting Antiretroviral Response against HIV-1

Chukwuemika Aroh, Zhaohui Wang, Nicole Dobbs, Min Luo, Zhijian Chen, Jimming Gao and Nan Yan

*J Immunol* 2017; 199:3840-3848; Prepublished online 30 October 2017;  
doi: 10.4049/jimmunol.1700972  
<http://www.jimmunol.org/content/199/11/3840>

---

**Supplementary Material** <http://www.jimmunol.org/content/suppl/2017/10/28/jimmunol.1700972.DCSupplemental>

### Why *The JI*?

- **Rapid Reviews!** 30 days\* from submission to initial decision
- **No Triage!** Every submission reviewed by practicing scientists
- **Speedy Publication!** 4 weeks from acceptance to publication

\*average

**References** This article **cites 26 articles**, 5 of which you can access for free at: <http://www.jimmunol.org/content/199/11/3840.full#ref-list-1>

**Subscription** Information about subscribing to *The Journal of Immunology* is online at: <http://jimmunol.org/subscription>

**Permissions** Submit copyright permission requests at: <http://www.aai.org/About/Publications/JI/copyright.html>

**Email Alerts** Receive free email-alerts when new articles cite this article. Sign up at: <http://jimmunol.org/alerts>



# Innate Immune Activation by cGMP-AMP Nanoparticles Leads to Potent and Long-Acting Antiretroviral Response against HIV-1

Chukwuemika Aroh,<sup>\*,†,1</sup> Zhaohui Wang,<sup>†,1</sup> Nicole Dobbs,<sup>\*</sup> Min Luo,<sup>†</sup> Zhijian Chen,<sup>‡,§,2</sup> Jinming Gao,<sup>†,¶,||,2</sup> and Nan Yan<sup>\*,#,2</sup>

HIV-1 evades immune detection by the cGAS-STING cytosolic DNA-sensing pathway during acute infection. STING is a critical mediator of type I IFN production, and STING agonists such as cGMP-AMP (cGAMP) and other cyclic dinucleotides elicit potent immune and antitumor response. In this article, we show that administration of cGAMP, delivered by an ultra-pH-sensitive nanoparticle (NP; PC7A), in human PBMCs induces potent and long-acting antiretroviral response against several laboratory-adapted and clinical HIV-1 isolates. cGAMP-PC7A NP requires endocytosis for intracellular delivery and immune signaling activation. cGAMP-PC7A NP-induced protection is mediated through type I IFN signaling and requires monocytes in PBMCs. cGAMP-PC7A NPs also inhibit HIV-1 replication in HIV<sup>+</sup> patient PBMCs after ex vivo reactivation. Because pattern recognition receptor agonists continue to show more clinical benefits than the traditional IFN therapy, our data present important evidence for potentially developing cGAMP or other STING agonists as a new class of immune-stimulating long-acting antiretroviral agents.

*The Journal of Immunology*, 2017, 199: 3840–3848.

Human cells detect invading pathogens with pattern recognition receptors (PRRs) that activate the production of type I IFNs (IFN-Is). IFN-Is initiate immediate cell-intrinsic antiviral response to contain the pathogen as well as adaptive immune response to achieve long-term protection (1). To counteract this immune surveillance, many viruses have evolved strategies to evade innate immune detection. We showed previously that HIV-1 exploits host DNase TREX1 to prevent cytosolic DNA sensing, and that *Trex1* deficiency allows accumulation of HIV-1 reverse-transcribed DNA that can be detected by the cGAS-STING pathway (2, 3). TREX1 knockdown in vaginal tissue ex-

plant and in humanized mice also results in elevated IFN-I response to acute HIV-1 infection and reduced viral replication and disease (4). Other studies in recent years have uncovered additional mechanisms of HIV-1 immune evasion, by exploiting host proteins such as SAMHD1 and CPSF6, in a variety of immune cell types (5). Overcoming HIV immune evasion allows for robust sensing of HIV-1 in CD4 T cells, macrophages, and myeloid dendritic cells, maturation of infected myeloid dendritic cells, production of IFN, and activation of T cells in vitro (5, 6). A striking common scheme of many of these HIV-1 evasion mechanisms is to prevent activation of the cGAS-STING pathway, indicating the importance of this pathway in immune detection of HIV-1 and presenting potential therapeutic opportunities for exploiting this pathway.

Upon DNA binding in the cytosol, cGAS is activated and produces the cyclic dinucleotide cGMP-AMP (cGAMP). cGAMP then binds to the adaptor protein STING on the endoplasmic reticulum, which recruits the kinase TBK1 and the transcription factors NF-κB and IFN regulatory factor 3 (IRF3), leading to activation of IFN-I and inflammatory responses. cGAMP has unique properties of being a small molecule (dinucleotide) and a potent activator of STING signaling, and it has been demonstrated as a potent adjuvant to elicit Ab and T cell responses in mice (7). In clinical settings (e.g., cancer), PRR agonists are becoming preferred therapy over IFNs, because of their superior pharmacokinetics, ability to induce other immunoregulatory cytokines in addition to IFNs, and better toxicity profiles (8).

Although some cells can take up free cGAMP and cGAMP analogues *in vivo* (7, 9, 10), cytosolic delivery of naked cGAMP is still challenging, likely because of the inherent dual negative charges of cGAMP and the presence of an extracellular enzyme that cleaves cGAMP (11). Multiple administrations of cGAMP are needed to achieve antitumor effects in mouse xenograft models. cGAMP also has never been evaluated as an antiretroviral therapy (ART). Recently, we have developed a series of ultra-pH-sensitive nanoparticles (UPS NPs) with tunable, exquisitely sharp pH response arising from catastrophic phase transitions during pH-triggered

\*Department of Immunology, University of Texas Southwestern Medical Center, Dallas, TX 75390; <sup>†</sup>Simmons Comprehensive Cancer Center, University of Texas Southwestern Medical Center, Dallas, TX 75390; <sup>‡</sup>Department of Molecular Biology, University of Texas Southwestern Medical Center, Dallas, TX 75390; <sup>§</sup>Howard Hughes Medical Institute, University of Texas Southwestern Medical Center, Dallas, TX 75390; <sup>¶</sup>Department of Pharmacology, University of Texas Southwestern Medical Center, Dallas, TX 75390; <sup>||</sup>Department of Otolaryngology, University of Texas Southwestern Medical Center, Dallas, TX 75390; and <sup>#</sup>Department of Microbiology, University of Texas Southwestern Medical Center, Dallas, TX 75390

<sup>1</sup>C.A. and Z.W. are cofirst authors.

<sup>2</sup>Z.C., J.G., and N.Y. are cosenior authors.

ORCIDs: 0000-0003-4972-5232 (C.A.); 0000-0003-1944-9740 (N.D.).

Received for publication July 10, 2017. Accepted for publication October 3, 2017.

This work was supported by the National Institutes of Health (Grant AI098569 to N.Y.), the National Institute of Biomedical Imaging and Bioengineering (Grant EB013149 to J.G.), and the Burroughs Wellcome Fund (to N.Y.).

Address correspondence and reprint requests to Dr. Nan Yan, Dr. Jinming Gao, or Dr. Zhijian Chen, University of Texas Southwestern Medical Center, 6000 Harry Hines Boulevard, Dallas, TX 75390. E-mail addresses: nan.yan@UTSouthwestern.edu (N.Y.), jinming.gao@UTSouthwestern.edu (J.G.), or zhijian.chen@UTSouthwestern.edu (Z.C.).

The online version of this article contains supplemental material.

Abbreviations used in this article: ART, antiretroviral therapy; cGAMP, cGMP-AMP; D<sub>h</sub>, hydrodynamic diameter; DLS, dynamic light scattering; IFN-I, type I IFN; IRF3, IFN regulatory factor 3; ISG, IFN-stimulated gene; NP, nanoparticle; PRR, pattern recognition receptor; qRT-PCR, quantitative RT-PCR; RTase, reverse transcriptase; THF, tetrahydrofuran; UPS NP, ultra-pH-sensitive nanoparticle.

Copyright © 2017 by The American Association of Immunologists, Inc. 0022-1767/17/\$35.00

self-assembly of amphiphilic block copolymers (12). These NPs can serve as carriers for therapeutic cargos and achieve cytosolic delivery of protein Ags for the activation of tumor-specific T cells (13). In this study, we evaluated the use of multiple UPS NP compositions to enhance cytosolic delivery of cGAMP into cells, and discovered that cGAMP-PC7A NP elicits potent and long-acting inhibition of multiple HIV-1 isolates in human PBMCs. We also elucidated the mechanism of cGAMP-PC7A NP-mediated immune protection and demonstrated its efficacy in PBMCs isolated from HIV<sup>+</sup> individuals.

## Materials and Methods

### Cells and viruses

PBMCs from anonymous healthy donors were isolated from blood purchased from Carter Bloodcare, a local blood bank, usually on the same day of blood draw. Peripheral immune cells were isolated using Ficoll Plaque Centrifugation at 1700 rpm for 30 min, and lysis of contaminating RBCs was removed by resuspension of PBMCs in ACK lysis buffer (Life Technologies) for 15 min on ice. PBMCs were maintained without stimulation in RPMI 1640 medium supplemented with 10% (v/v) FBS and 2 mM L-glutamine (Sigma-Aldrich), 10 mM HEPES (Sigma-Aldrich), 1 mM sodium pyruvate (Sigma-Aldrich), 100 U/ml penicillin (Sigma-Aldrich), and 100 mg/ml streptomycin (Sigma-Aldrich) at 37°C and 5% CO<sub>2</sub>. Consenting HIV<sup>+</sup> patients were recruited according to Institutional Review Board-approved protocols, and their PBMCs were similarly isolated and cultured as described earlier. Human studies are approved by University of Texas Southwestern Medical Center Institutional Review Board.

Cell viability was determined using Fixable Red Dead Cell stain kit (Life Technologies) using 0.5 µl of dye to stain cells in 1 ml of PBS for 5 min in the dark. These were then washed twice with PBS and measured on FACSCalibur. As a positive control for dead cells, PBMCs were boiled at 95°C for 20 min and also stained with the same procedure to determine the peak of dead cells.

CD4<sup>+</sup> T cells, B cells, and monocytes were positively selected using Miltenyi Biotec human microbeads against CD4<sup>+</sup> (130-045-101), CD19<sup>+</sup> (130-050-301), and CD14<sup>+</sup> (130-050-201) according to the manufacturer's recommendations. The labeled cells typically had purity >90%. For depletion experiments, the same isolation protocol was used, but now the flow-through PBMCs were taken; we regularly achieved >95% depletion for monocyte and B cells.

To analyze HIV receptor and coreceptor expression, we isolated CD4<sup>+</sup> T cells and CD14<sup>+</sup> monocytes by positive selection using microbeads (Miltenyi). These cells were then treated with 2 µg/ml cGAMP-PC7A for 2 d. After treatment, the cells were collected, fixed, and stained with CCR5, CD4, CXCR4 Abs. Flow cytometry was used to determine the mean fluorescence intensity compared with PC7A alone treatment.

HIV strains (BaL, IIIB) were propagated in U937 cell lines, concentrated using Amicon Ultra-15 centrifugal filter units (Millipore), and titrated by quantitative PCR-based product-enhanced reverse transcriptase assay described later. The HIV LAI strain was obtained from NIH AIDS reagent program (catalog no. 2522), amplified in PBMCs, and concentrated using LentiX concentrator (Clontech) according to the manufacturer's recommendation.

### HIV-1 titer quantitative PCR-based product-enhanced reverse transcriptase assay

As was previously described (14, 15), this assay uses reverse transcriptase (RTase) activity in the sample to power a quantitative RT-PCR (qRT-PCR), with the quantity of accumulated product serving as a proxy for viral concentration. Viral particles in the supernatant are lysed by mixing 1:1 with lysis buffer for 10 min at room temperature. The reaction is quenched by adding nuclease-free water (nine times lysate volume) to lysate. This diluted lysate (6 µl) is added to a MicroAmp fast 96-well reaction plate (Applied Biosystems) along with 1:10 diluted Roche MS2 RNA (1 µl), 10 µM Sigma MS2 Fwd (1 µl) and Rev primers (1 µl), 1:10 diluted Invitrogen RNaseOUT (1 µl), and Bio-Rad Sybr green (10 µl) for each sample. All dilutions were done in nuclease-free water (Ambion). These samples are then vortexed and spun down, before running on a AB 7500 Fast Real Time PCR System using the following program: 1) 42°C for 20 min; 2) 95°C for 5 min; 3) 95°C for 3 s; 4) 60°C for 30 s and plate read; and 5) repeat from step 3, 39 times. To normalize measurements across different plates, we included aliquots from one HIV-1 stock in all plates, and its measurement was used to divide the values in the experimental conditions.

### Syntheses of PEG-b-PR block copolymers

PEG-b-PR copolymers were synthesized by atom transfer radical polymerization following similar procedures previously reported (16). The dye-free copolymers were used in polymer characterizations. PEG-b-PC7A is used as an example to illustrate the procedure. First, C7A-MA (1.48 g, 7 mmol), PMDETA (21 µl, 0.1 mmol), and MeO-PEG<sub>114</sub>-Br (0.5 g, 0.1 mmol) were charged into a polymerization tube. Then a mixture of 2-propanol (2 ml) and DMF (2 ml) was added to dissolve the monomer and initiator. After three cycles of freeze-pump-thaw to remove the oxygen, we added CuBr (14 mg, 0.1 mmol) into the polymerization tube under nitrogen atmosphere, and the tube was sealed in vacuo. The polymerization was carried out at 40°C for 10 h. After polymerization, the reaction mixture was diluted with 10 ml of tetrahydrofuran (THF) and passed through a neutral Al<sub>2</sub>O<sub>3</sub> column to remove the catalyst. The THF solvent was removed by rotovap. The residue was dialyzed in distilled water and lyophilized to obtain a white powder. After synthesis, the polymers were characterized by <sup>1</sup>H nuclear magnetic resonance and gel permeation chromatography.

### Preparation of micelle NPs

cGAMP-loaded micelles were prepared following a solvent evaporation method. In the example of PEG-b-PC7A, both the copolymer (10 mg) and cGAMP (1 mg) were first dissolved in 1 ml of methanol and then added into 4 ml of distilled water dropwise under sonication. The mixture was filtered four times to remove THF using the microultrafiltration system (molecular mass = 100 kDa). The filtrate was collected and cGAMP was quantified by UV-Vis spectrometer at 258 nm. After micelle formation, the NPs were characterized by dynamic light scattering (DLS; Malvern MicroV model; He-Ne laser,  $\lambda$  = 632 nm) for hydrodynamic diameter (D<sub>h</sub>). The control unloaded NPs were prepared with same protocol as described earlier, except the addition of cGAMP into the methanol. All NPs were directly added into the culture medium for delivery into cells.

To evaluate the loading stability, we stored the micelle NPs in 4°C for 1 wk. The size and cGAMP encapsulation efficiency were measured by DLS and ultrafiltration method, respectively.

To study PC7A NP uptake mechanism, we labeled PC7A NP with Cy5 dye (PC7A-Cy5). PBMCs from healthy donors were pretreated with endocytosis or endolysosome inhibitors for 1 h and then treated with PC7A-Cy5 for 4 h. The cells were then collected, washed extensively, and fixed. Activation of Cy5 fluorescence signals within cells was quantified by flow cytometry as an indication of NP dissociation. Similarly, PBMCs from healthy donors were pretreated with endocytosis or endolysosome inhibitors for 1 h and then treated with 2 µg/ml cGAMP-PC7A for 6 h. The cells were then collected in TRIzol; RNA was isolated for qRT-PCR for induction of immune response genes.

### qRT-PCR, Milliplex, and Western blots

Cytokine mRNA was extracted from cells using TR1 Reagent (Sigma-Aldrich), and cDNA was generated using iSCRIPT master mix (Bio-Rad). Quantitative PCR was run using specific primers (Bio-Rad) and normalized relative to *Gapdh* mRNA. HIV patient cytokine mRNA profiles were determined using Prime PCR custom plates (Bio-Rad) using their recommended primers against our genes of interest.

Proteins of select cytokines in the culture supernatant were collected and measured using Luminex xMAP technology and a human Milliplex kit (Millipore).

For Western blots, primary Abs used were rabbit anti-TBK (Cell Signaling), rabbit anti-IRF3 (Cell Signaling), rabbit anti-STING (Cell Signaling), rabbit anti-phospho TBK (Ser172) clone D52c2 (Cell Signaling), rabbit anti-HMGB2 (Abcam), and mouse anti-tubulin (Sigma-Aldrich) according to blotting procedures previously described (17). All sample loadings were normalized to total protein measured by the BCA assay.

### Statistical analysis

Statistical significance was determined using a two-tailed Student *t* test analysis available on GraphPad Prism 6. The *p* values <0.05 were considered significant.

## Results

### Formulation and characterization of cGAMP UPS NPs

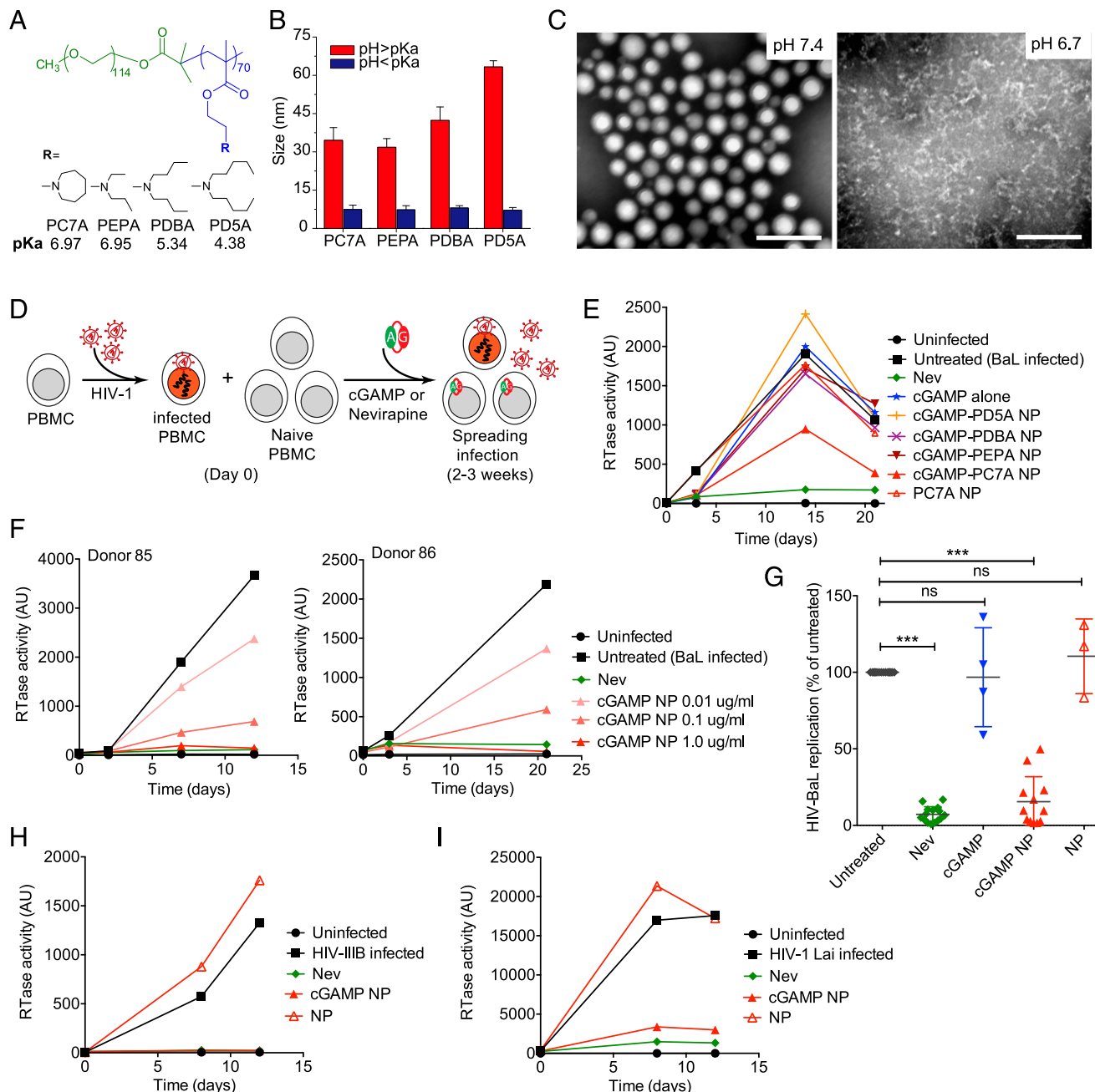
Cytosolic delivery of cGAMP is challenging due to its membrane-impermeable property as a result of dual negative charges. In this study, we used the UPS NP with exquisite pH response to the endolysosomal environment to deliver cGAMP into cells (Fig. 1A,

Table I). UPS-PC7A NPs allowed for >2-fold higher loading of cGAMP over the other UPS copolymers with linear side chains (Table II), potentially because of the more favorable hydrophobic interactions (i.e., guanidine and adenine bases with cyclic alkyl groups on the tertiary amines) and internal salt-bridge (i.e., cGAMP phosphates to ammonium groups in the UPS copolymer). The resulting cGAMP-NPs were stable during storage (no cGAMP release over 7 d) (Table II). At pH 7.4, UPS NPs were present as self-assembled micelles with a diameter of 30–70 nm and a spherical

morphology (Fig. 1B, 1C). Micelle dissociates into unimers at pH values less than  $pK_a$ , resulting in efficient cGAMP release.

## *cGAMP-PC7A NP elicits potent antiretroviral response against clinical HIV-1 isolates in human PBMCs*

To determine whether activation of STING signaling by cGAMP-NPs could induce protective antiviral response against HIV-1 infection, we performed the HIV-1 spreading assay using human PBMCs isolated from healthy donors. We first infected PBMCs



**FIGURE 1.** cGAMP-PC7A NPs elicit potent antiretroviral response against HIV-1 in human PBMCs. **(A)** Structures of the UPS copolymers. **(B)** Size changes of cGAMP-loaded micelle NPs in buffers at pH greater than or less than pKa ( $n = 3$ ). **(C)** Transmission electron micrograph images of cGAMP-loaded PEG-*b*-PC7A NPs at pH 7.4 and 6.7. Scale bars, 100 nm. **(D)** A schematic diagram of HIV-1 spreading assay in PBMCs. **(E)** HIV-BaL replication in PBMCs treated with indicated reagents (right). All NPs were used at 1  $\mu$ g/ml. **(F)** HIV-BaL replication in PBMCs treated with increasing amount of cGAMP-NP (PC7A, same below). Two representative donors are shown. **(G)** HIV-BaL replication in PBMCs treated with the indicated reagents (x-axis): cGAMP was used at 1  $\mu$ g/ml. cGAMP-NP was used at 1  $\mu$ g/ml, and equivalent amount of NP alone was used as control. Each data point represents an individual donor. **(H and I)** HIV-IIIB (H) or HIV-LAI (I) replication in PBMCs treated with Nev or cGAMP-NP. Assay performed as illustrated in (D). Data are representative of at least three independent experiments with independent donors. Error bars represent SEM. \*\*\* $p < 0.005$ , Student *t* test. Nev, nevirapine (4  $\mu$ M, same throughout).

Table I. Chemical compositions and physical properties of UPS NPs

Polymer	Monomer	Mn (kDa) <sup>a</sup>	PDI <sup>a</sup>	pKa <sup>b</sup>	D <sub>h</sub> (nm) <sup>c</sup>
PC7A	C7A-MA	20.9	1.29	6.97	30.1 ± 7.1
PEPA	EPA-MA	20.2	1.12	6.95	28.6 ± 2.0
PDBA	DBA-MA	22.1	1.12	5.34	45.6 ± 9.6
PD5A	D5A-MA	21.1	1.17	4.38	59.8 ± 3.5

<sup>a</sup>Number-averaged molecular mass (Mn) and polydispersity index (PDI) were determined by gel permeation chromatography using THF as the eluent.

<sup>b</sup>pKa was determined by pH titration of polymer solutions using 4 M NaOH.

<sup>c</sup>Size was measured using DLS, mean ± SD.

with a replication-competent HIV-BaL strain in bulk for 5–7 d. Then, infected PBMCs were washed (to remove free viruses) and split into several conditions where we added uninfected naive PBMCs from the same donor (“reseeding”) to allow HIV spreading (Fig. 1D). Different treatments were administered at the point of reseeding (day 0). We then followed the growth of HIV-1 by measuring HIV-1 RTase activity in the media (see *Materials and Methods*). HIV-BaL titer increased steadily in PBMCs after reseeding for approximately 2 wk before starting to decline (Fig. 1E). As a positive control, RTase inhibitor nevirapine completely inhibited HIV-BaL spreading in PBMCs. When we compared cGAMP-NPs releasing at different pHs ranging from 4.38 to 6.97, only cGAMP-PC7A NP (transition pH 6.97) inhibited HIV-BaL spreading (Fig. 1E), but not with other copolymers with less endosomolytic ability for cytosolic delivery of encapsulated cargos (16). Neither PC7A NP alone nor naked cGAMP inhibited HIV-BaL replication. We also found that cGAMP-PC7A NP (we will call cGAMP-NP later) induced protection against HIV-BaL in a dose-dependent manner in PBMCs isolated from multiple donors (Fig. 1F, 1G). cGAMP-NP did not induce appreciable cytotoxicity in PBMCs at the dose needed for full protection (Supplemental Fig. 1A). We also tried to deliver cGAMP complexed with lipid NPs (Lipofectamine 2000), and observed similar dose-dependent protection against HIV-BaL in PBMCs without cytotoxicity (Supplemental Fig. 1B, 1C), although a much higher amount of cGAMP-Lipo is needed to achieve a similar level of antiretroviral response as cGAMP-NP. We also compared cGAMP-NP and cGAMP-Lipo in THP-1 cells and found that cGAMP-NP is much more potent at eliciting IFN and IFN-stimulated genes (ISGs) compared with cGAMP-Lipo (Supplemental Fig. 1D).

cGAMP-NP also did not alter HIV receptor CD4 and coreceptor CXCR4 and CCR5 expression in CD4<sup>+</sup> T cells isolated from healthy donor PBMCs (Supplemental Fig. 2A). cGAMP-NP-treated CD14<sup>+</sup> monocytes decreased CD4, but not CXCR4 or CCR5, expression after 2 d (Supplemental Fig. 2B). PC7A NP releases content during early stages of endocytosis (18). To determine whether endocytosis or acidified endolysosome is required for intracellular delivery and immune activation by cGAMP-PC7A NP in PBMCs, we pretreated PBMCs with dynasore that inhibits clathrin-mediated endocytosis or with chloroquine to

block acidification of endolysosomes. We then added PC7A-Cy5 NP to the culture media and measured intracellular delivery by FACS. In a separate experiment, we added cGAMP-PC7A NP to the cells and measured CXCL10 expression. We found that dynasore treatment potently blocked PC7A-Cy5 NP delivery and cGAMP-PC7A NP-mediated immune activation, whereas chloroquine did not, suggesting that endocytosis is critical for cGAMP-PC7A NP delivery of cGAMP into the cell (Supplemental Fig. 2C, 2D).

HIV-BaL is an M-tropic R5 strain. We next infected PBMCs with two other T-tropic X4 strains of HIV-1, IIIB, and LAI. cGAMP-NP inhibited spreading of both strains in PBMCs (Fig. 1H, 1I). Together, we conclude that cGAMP-NP inhibits replication-competent HIV-1 spreading in PBMCs, and that cGAMP-mediated antiretroviral response can achieve similar potency as RTase inhibitors *in vitro*.

*cGAMP-NP-induced protective immune response against HIV-1 is mediated through IFN-I signaling*

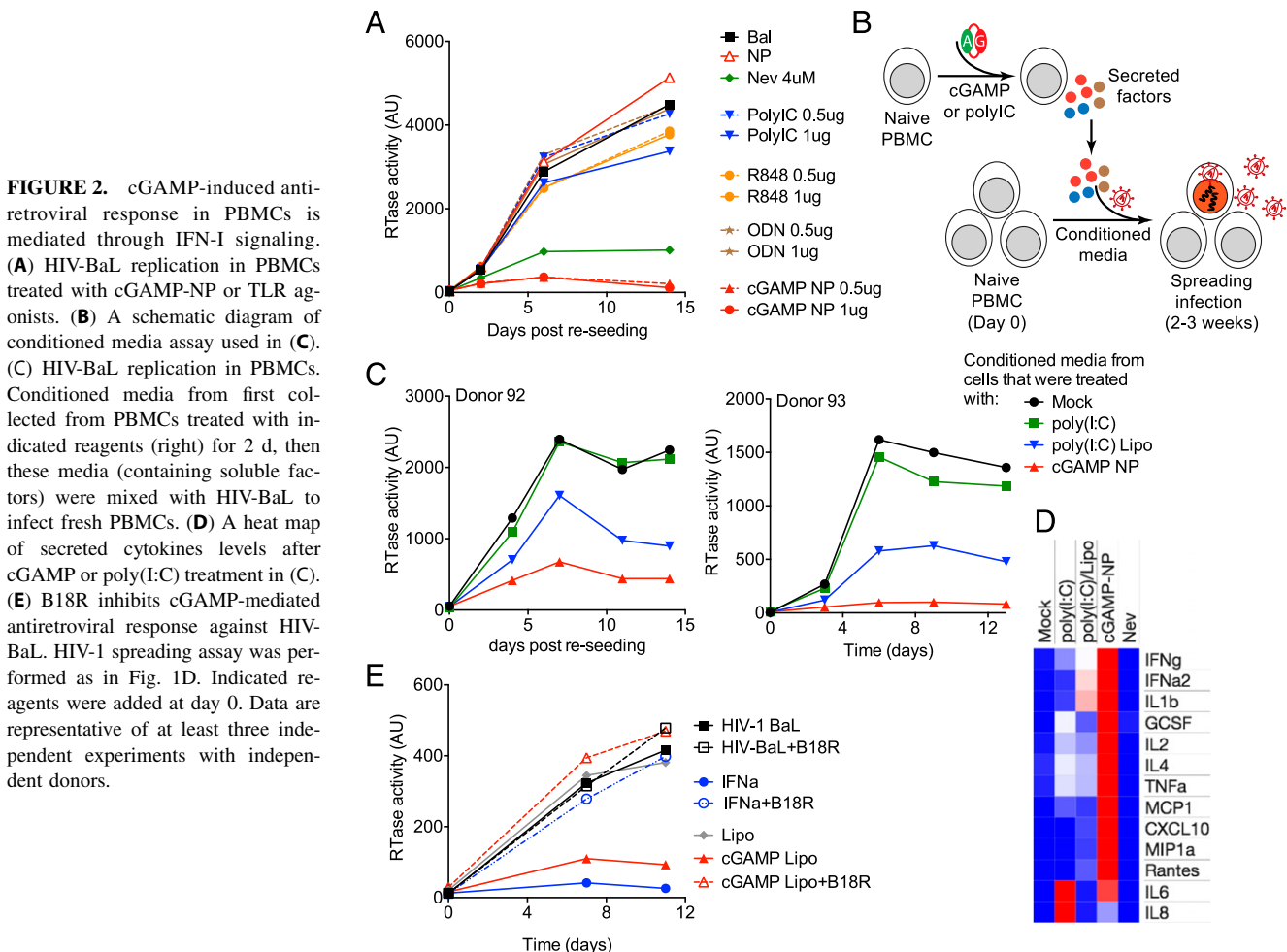
We next compared cGAMP-NP with TLR3 agonist poly(I:C), TLR7/8 agonist R848, and TLR9 agonist oligodeoxynucleotides containing CpG motifs in the HIV-1 spreading assay. Many of these TLR agonists induce potent inflammatory responses, which we confirmed in PBMCs by qRT-PCR (data not shown). We found that none of the TLR agonists elicited detectable protection against HIV-BaL replication in PBMCs (Fig. 2A). To determine whether cGAMP-induced protection is mediated through soluble factors, we next compared cGAMP-NP with extracellularly versus intracellularly delivered poly(I:C) (complexed with Lipofectamine, activates the cytosolic RIG-like receptor pathway) in the “conditioned media” experiment (Fig. 2B). We first treated PBMCs with cGAMP-NP, poly(I:C) alone, or poly(I:C)-Lipo, and washed cells extensively 2 d later to remove excess agonists that were not taken up by cells. We then incubated stimulated PBMCs in fresh media for 3 d to collect secreted soluble factors. We added the conditioned media together with HIV-BaL to fresh PBMCs to examine whether they can confer protection against HIV-BaL replication. Conditioned media from cGAMP-NP-treated cells strongly inhibited HIV-BaL replication, suggesting that soluble factors are largely responsible for cGAMP-NP-mediated protection (Fig. 2C). Media from poly(I:C)-treated cells did not confer

Table II. Characterization of cGAMP-loaded USP NPs in water

NPs	Time 0		1 wk	
	D <sub>h</sub> (nm) <sup>a</sup>	EE% <sup>b</sup>	D <sub>h</sub> (nm)	EE%
cGAMP-PC7A NP	34.5 ± 5.0	69.7	32.8 ± 5.5	69.5
cGAMP-PEPA NP	31.8 ± 3.4	33.4	32.7 ± 3.3	33.4
cGAMP-PDBA NP	42.3 ± 5.3	26.3	43.7 ± 6.9	26.2
cGAMP-PD5A NP	63.3 ± 2.4	38.5	64.6 ± 4.1	38.5

<sup>a</sup>Size was measured using DLS, mean ± SD.

<sup>b</sup>Encapsulation efficiency (EE) was measured by the ultrafiltration method.



any protection, and media from poly(I:C)-Lipo–treated cells conferred only partial protection. We also analyzed cytokines secreted by PBMCs treated with poly(I:C), poly(I:C)-Lipo, cGAMP-NP, or nevirapine (Fig. 2D). As expected, poly(I:C) induced a predominant inflammatory response and poly(I:C)-Lipo induced a predominant IFN response. In contrast, cGAMP-NP induced strong response in both IFN and inflammatory cytokines. We next investigated the role of IFN-I signaling in cGAMP-mediated protection against HIV-1 infection. Both rIFN- $\alpha$  and cGAMP-Lipo induced potent protection against HIV-BaL spreading in PBMCs, and in both cases the protection was completely reversed by an IFN- $\alpha/\beta$  receptor inhibitor, B18R, suggesting that the IFN signaling pathway plays a key role in cGAMP-NP–mediated protection (Fig. 2E).

#### cGAMP-induced protective immune response in human PBMCs is dependent on monocytes

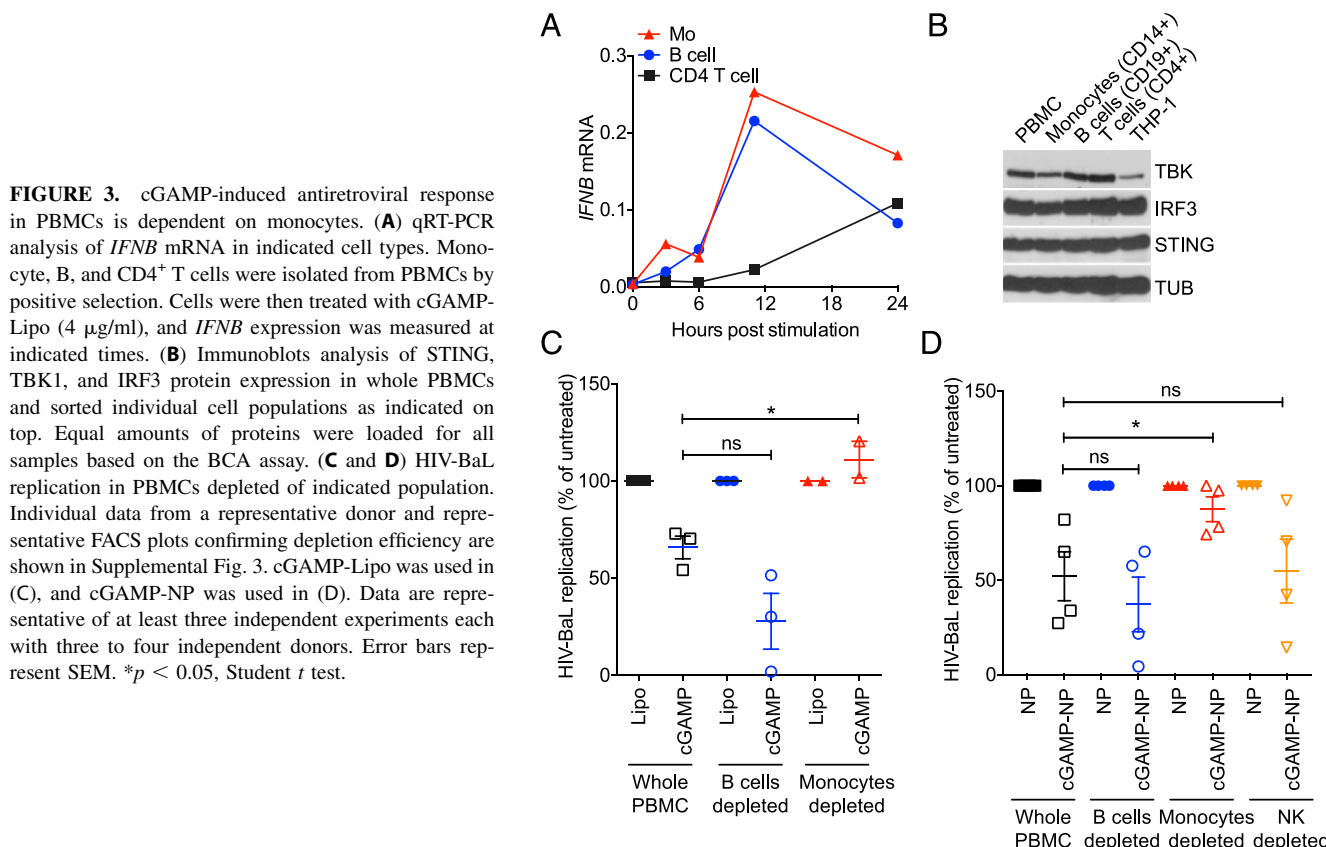
We next tried to determine the immune cell type in PBMCs that is responsible for cGAMP-induced protection against HIV-1 infection. We first characterized the signaling kinetics activated by cGAMP in positively selected immune cell populations. cGAMP induced robust IFN- $\beta$  expression in CD19 $^+$  B cells and CD14 $^+$  monocytes during the first 12 h followed by gradual decline, likely because of cell-intrinsic mechanisms to prevent excessive IFN activation (Fig. 3A). In contrast, CD4 $^+$  T cells presented a much slower kinetics of IFN- $\beta$  expression after cGAMP stimulation, with IFN- $\beta$  mRNA becoming detectable after 6 h and continued to increase up to 24 h. All immune cell types express similar levels of endogenous STING, TBK1, and IRF3 proteins analyzed by Western blot (normalized to total protein) (Fig. 3B). HIV-1 rep-

lication in CD4 $^+$  T cells in PBMCs. We next depleted B cells, monocytes, or NK cells with magnetic beads from whole PBMCs and evaluated HIV-1 replication with and without cGAMP-Lipo or cGAMP-NP stimulation (Fig. 3C, 3D, Supplemental Fig. 3A–D). We found that cGAMP-mediated protection was completely lost in monocyte-depleted PBMCs, regardless of Lipo or NP delivery, whereas B cell or NK cell depletion had little or no effect (Fig. 3C, 3D). We confirmed the depletion by FACS (Supplemental Fig. 3D). We also analyzed STING signaling activation in PBMCs or monocytes by immunoblots (Supplemental Fig. 3E). The kinetics of TBK1 phosphorylation in both cell cultures are similar, consistent with monocytes being the primary mediators of cGAMP-induced protection against HIV-1.

We next compared cGAMP with another STING against c-di-GMP (both delivered by Lipo) at stimulating immune gene expression in PBMCs and a monocyte cell line THP-1 cells. cGAMP binds to STING at a much higher affinity compared with c-di-GMP (19). We found that cGAMP also stimulated more robust immune response compared with c-di-GMP in PBMCs and THP-1 cells (Fig. 4). Collectively, these data suggest that monocytes are the key immune cell population in PBMCs that are mediating cGAMP-induced protection against HIV-1 infection. Our data also demonstrate that mammalian cGAMP is more potent than bacterial cyclic dinucleotides at stimulating immune responses in human PBMCs.

#### cGAMP-NP elicits long-acting antiretroviral response against HIV-1 replication and spreading

One of the challenges facing current ART is patient adherence. Most conventional antiretroviral regimens require daily dosing of a



combination of antiretroviral drugs, and lapses in treatment often lead to rapid rebound of viral load. Thus, long-acting ARTs represent a major need for HIV/AIDS. Several candidates based on slow-release formulation of current and new ARTs are in advance development (20). To determine whether cGAMP-NP can elicit long-acting inhibition of HIV-1 replication and spreading by activating sustained immune responses, we performed the extended HIV-1 spreading assay interrupted by a “media wash” that simulates treatment interruption and clearance of the initial antiretroviral drug (Fig. 5A). The first stage of the assay is identical to the HIV-1 spreading assay described earlier, where HIV-BaL–infected PBMCs were cocultured with naive PBMCs in the presence or absence of various treatments. After 7 d, we washed the cells and changed fresh media (to remove drugs and viruses), at which time we also added more naive PBMCs and followed HIV-1 spreading for three more weeks. We found that both nevirapine and cGAMP-NP inhibited HIV-1 replication before treatment interruption (media wash; Fig. 5B). After treatment interruption, viral load in both untreated and nevirapine-treated samples increased quickly, rising to the level similar to the untreated condition before treatment interruption (Fig. 5B). This rapid viral load rebound after ART treatment interruption closely resembles the clinical observation of HIV-1–infected patients experiencing a lapse in treatment. Remarkably, cGAMP-NP–treated samples remained inhibited with low viral load up to 3 wk after media wash in PBMCs isolated from multiple healthy donors (Fig. 5B, 5C). We also measured cytokines produced during the course of “long-acting” experiments. HIV-1 infection with and without nevirapine treatment in PBMCs produced several inflammatory cytokines (e.g., IL-6, IL-8, G-CSF, TNF- $\alpha$ ), but not IFNs (IFN- $\alpha$ 2, IFN- $\gamma$ ) in the media (Supplemental Fig. 4A). In contrast, HIV-1–infected PBMCs treated with cGAMP-NP produced IFN and inflammatory cytokines. IFN- $\alpha$ 2 and MIP-1 $\alpha$  (an ISG) are also

continuously being produced at high levels in cGAMP-NP-treated cells more than 2 wk after the single treatment (Supplemental Fig. 4B). We also found that coadministration of B18R abolished cGAMP-NP-mediated long-acting protection (Fig. 5D) and no evidence of excessive cytotoxicity during the entire course of cGAMP treatment in multiple donors (data not shown). These data suggest that cGAMP induces a durable protective immune response in PBMCs against HIV-1 infection and replication that is largely dependent on IFN- $\lambda$ .

## *cGAMP-NP inhibits HIV-1 replication in HIV patient PBMCS ex vivo*

We next evaluated cGAMP-NP in HIV patient PBMCs ex vivo. We recruited HIV<sup>+</sup> individuals who have detectable viral load (RNA copy > 50/ml) and CD4 T cells (count > 100/ml), treatment-naïve or treatment-experienced, but have not been on any anti-retroviral medication for a minimum of 30 consecutive days before specimen collection. We first measured basal immune gene expression in PBMCs isolated from four HIV<sup>+</sup> patients and three healthy controls and how they respond to cGAMP-NP stimulation. All healthy control and HIV<sup>+</sup> patient PBMCs express low levels of IFN genes (e.g., IFN- $\alpha$ 4, IFN- $\beta$ 1), ISGs (e.g., CXCL10, IFIT1, OASL, etc.), and inflammatory genes (e.g., TNF- $\beta$ , IL-6, IL-8) (data not shown). cGAMP-NP induced comparable immune gene expression profiles in healthy control and HIV patient PBMCs (Fig. 6A).

We expect a substantial amount of HIV patient PBMCs to be latently infected, and would produce HIV-1 after PHA/IL-2 activation. We performed two assays (Fig. 6B, 6C). In the first assay, we waited 7 d after PHA/IL-2 activation to allow sufficient HIV production before treating cells with cGAMP-NP or antiretrovirals. In the second assay, we treated cells with cGAMP-NP or antiretrovirals immediately after PHA/IL-2 activation. We then

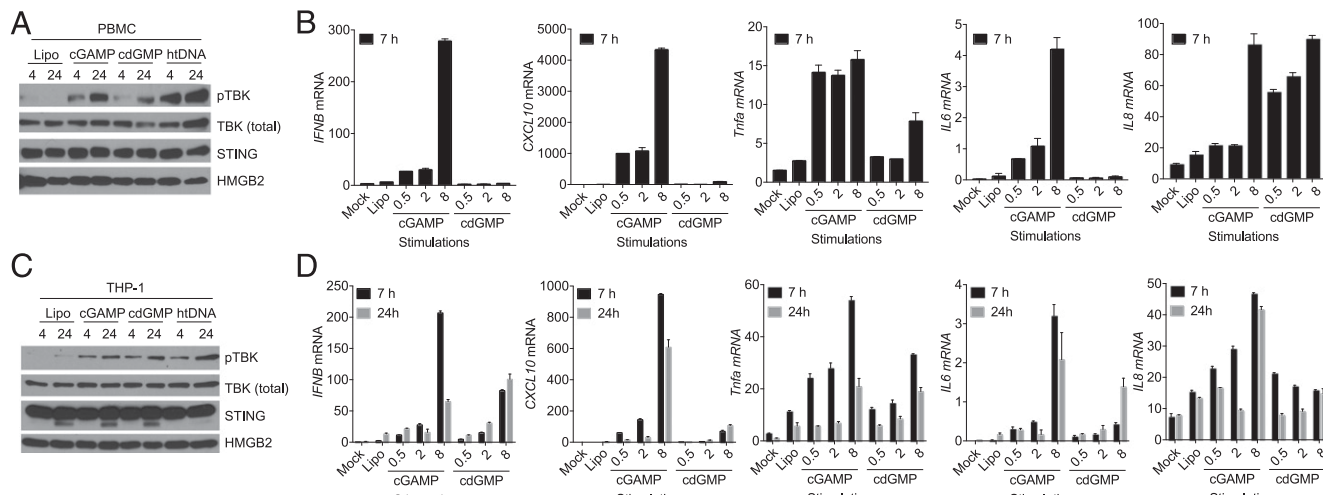


**FIGURE 4.** cGAMP is more potent than c-di-GMP at stimulating immune gene expression in PBMCs. **(A and B)** Immunoblots (A) and qRT-PCR analysis (B) of STING signaling activation in PBMCs by cGAMP (2  $\mu$ g/ml), c-di-GMP (2  $\mu$ g/ml), or herring testis DNA (1  $\mu$ g/ml). Cells were treated with the indicated ligand for 4, 7, or 24 h as indicated (4 and 24 h for immunoblots, 7 h for qRT-PCR). **(C and D)** Immunoblots (C) and qRT-PCR analysis (D) of STING signaling activation in THP-1 cells (monocyte cell line) by cGAMP (2  $\mu$ g/ml), c-di-GMP (2  $\mu$ g/ml) or herring testis DNA (1  $\mu$ g/ml). Cells were treated with the indicated ligand for 4, 7, or 24 h as indicated (4 and 24 h for immunoblots, 7 and 24 h for qRT-PCR). Data are representative of at least two independent experiments.

measured HIV replication after 1–2 wk. Antiretroviral drugs reduced HIV-1 replication overall in both assays, but not complete elimination, indicating that a substantial amount of latently infected cells in HIV patient PBMCs are producing HIV after reactivation. cGAMP-NP inhibited HIV replication at a similar efficacy as antiretrovirals when PBMCs were actively producing viruses, and cGAMP-NP potently inhibited HIV replication when cGAMP-NPs were administered immediately after reactivation (Fig. 6B, 6C). Together, given the distinct antiretroviral mechanism and long-acting benefit through stimulating the innate immune response, cGAMP-NP could be a desirable candidate as a new category of PRR-based long-acting ART.

## Discussion

Recent advances in understanding HIV-1 immune evasion mechanisms highlighted the importance of the cytosolic DNA-sensing cGAS-STING pathway in host immune response to HIV-1 infection. The same signaling pathway can be triggered by a small-molecule cGAMP that directly activates STING. We showed in this study that cGAMP-NP induced potent antiretroviral response against clinical HIV-1 isolates in PBMCs. Intracellular delivery of cGAMP is critical for inducing the protective immune response, as demonstrated by the lack of protection conferred by naked cGAMP. Among the NPs we tested, PC7A NP conferred the best antiretroviral activity over other NP compositions or lipofectamine. In

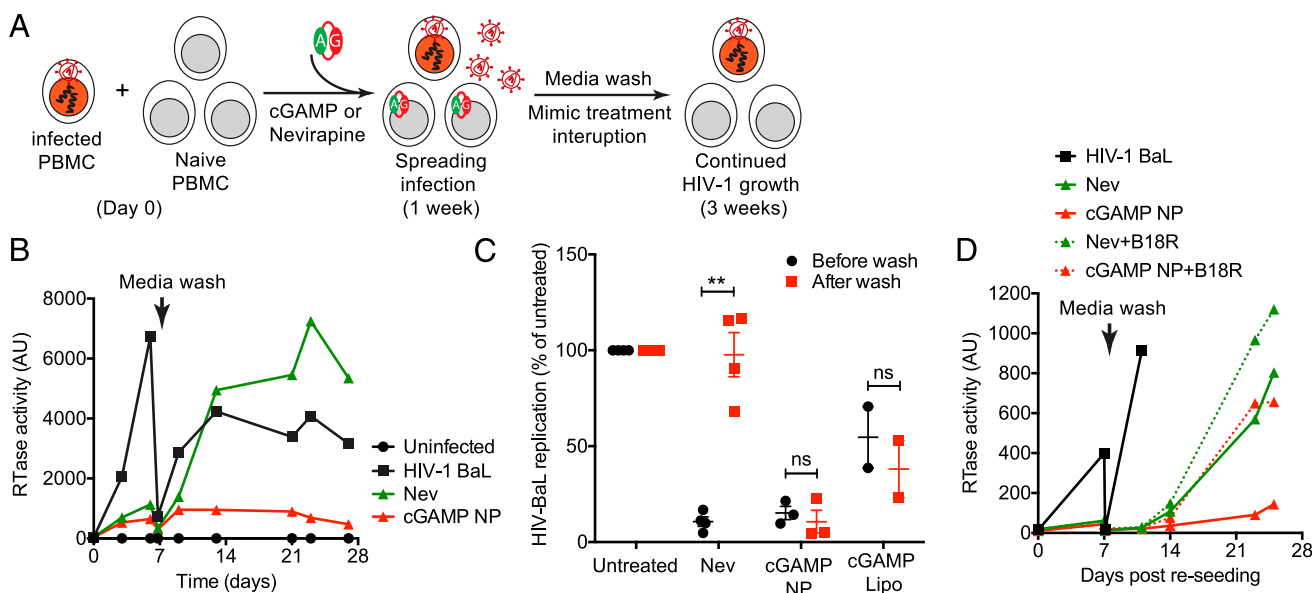


**FIGURE 5.** cGAMP-NP elicits long-acting antiretroviral response against HIV-1 in PBMCs. **(A)** A schematic diagram of modified HIV-1 spreading assay to include treatment interruption after 1 wk (long-acting experiment). **(B and C)** HIV-BaL replication in PBMCs treated with Nev (4  $\mu$ M) or cGAMP-NP (2  $\mu$ g/ml). Cells were washed with fresh media at day 7, and viral replication was continually monitored until day 27. One representative donor is shown in (B). Summary from multiple donors is shown in (C). **(D)** HIV-BaL replication in PBMCs treated with Nev (4  $\mu$ M) or cGAMP-NP (2  $\mu$ g/ml) with or without B18R (500 ng/ml). Experimental setup is similar to (B). Data are representative of at least three independent experiments with independent donors. Error bars represent SEM. \*\* $p$  < 0.01, Student  $t$  test.

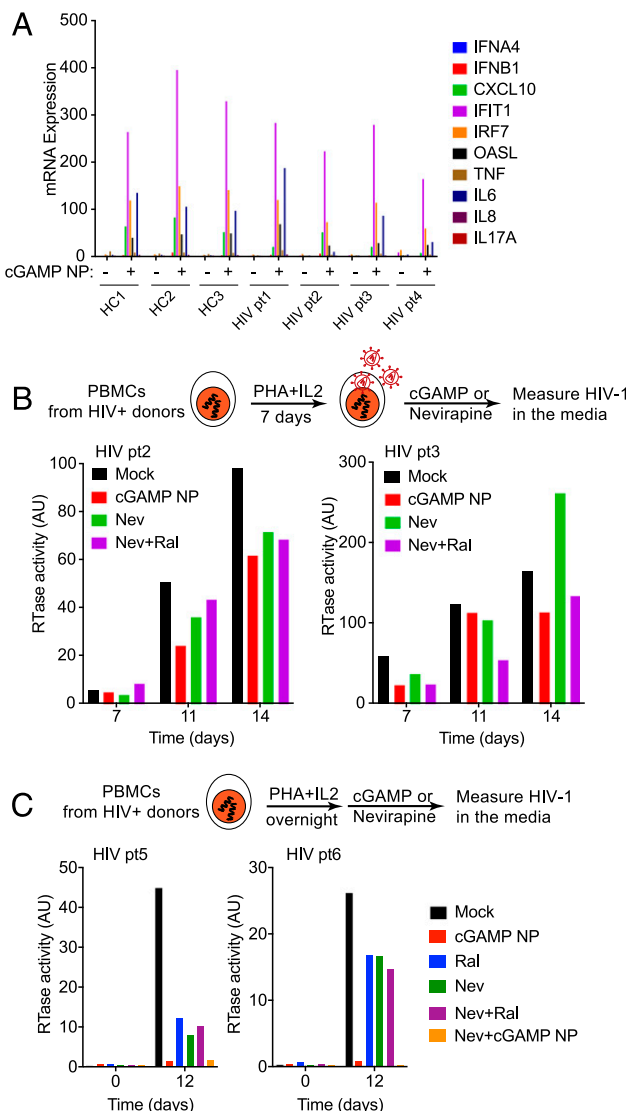


**FIGURE 6.** cGAMP-NP inhibits HIV-1 replication ex vivo. **(A)** qRT-PCR array analysis of indicated immune genes in PBMCs isolated from healthy or HIV<sup>+</sup> donors before and after cGAMP-NP treatment (2  $\mu$ g/ml) for 24 h.  $n = 3-4$ . **(B)** HIV-1 replication in patient PBMCs ex vivo after reactivation for 7 d and indicated treatment.  $n = 2$ . **(C)** HIV-1 replication in patient PBMCs ex vivo after reactivation overnight and immediately followed by indicated treatment. HIV replication was measured in the media at indicated days after reactivation.  $n = 2$ .

addition to the optimal pH transition (6.97) that targets the early endosomal pH for cGAMP release and the cyclic amine structure that facilitates the membrane disruption for cytosolic release (16), the direct binding of PC7A to the cytosolic domain of STING may also contribute to STING activation in addition to cGAMP. Indeed, recent studies in cGAS<sup>-/-</sup> knockout animals showed the cGAS-independent STING activation by PC7A NP alone in mice (13), although with a lesser magnitude compared with cGAMP. We did not observe antiretroviral activity in human PBMCs by PC7A NP alone. The combined cytosolic delivery of cGAMP and cGAS-independent STING activation by PC7A could confer a potential synergistic activation of STING to achieve maximal protection against HIV-1 infection.

Our study represents the first example, to our knowledge, of evaluating the potential of cGAMP as an ART for HIV-1. Because STING is a critical mediator of IFN production, STING agonists such as cGAMP and other cyclic dinucleotides are being devel-

oped as vaccine adjuvant to elicit potent immune response. STING signaling also elicits a strong antitumor response by boosting host immune recognition of tumor Ags (7, 10, 21, 22). We showed that cGAMP-NP induces potent antiretroviral response in human PBMCs, and the effect is long-acting. Several oral and injectable long-acting agents based on reformulation of ARTs are in advanced development with exciting potentials as pre-exposure prophylaxis or treatment (20, 23). The mechanism of cGAMP-NP-mediated antiretroviral activity is different from traditional ARTs or long-acting ART formulations, because cGAMP-NP acts by inducing a broad and sustained antiretroviral innate immune response. We defined that cGAMP-NP-mediated antiretroviral immune response in PBMCs is mediated by monocytes and IFN-I. Although we did not examine plasmacytoid dendritic cells in our depletion experiments, plasmacytoid dendritic cells are main producers of IFN-Is, and thus are likely to also contribute to the overall antiretroviral response elicited by cGAMP-NP. We also did not observe antiretroviral response from TLR agonists in the PBMC HIV-BaL spreading assay. One major difference between TLRs and STING signaling is that TLR expression is restricted to DCs and macrophages, whereas STING is ubiquitously expressed in almost all cell types. TLR- and STING-mediated signaling profiles are also different, which could contribute to their differential antiretroviral capacity. Interestingly, TLR agonist enhances latent HIV reactivation in vitro (24, 25), whereas we found cGAMP-NP inhibits HIV replication and possibly reactivation in PBMCs isolated from HIV<sup>+</sup> individuals.

Because PRR-based agonists are becoming more favorable therapeutics than rIFN with less toxicity and better immune response profile, our study presents an important proof of principle for harnessing cGAMP-mediated innate immune response for HIV-1 therapy. A recent study using aptamer-mediated siRNA knockdown of TREX1 in humanized mice, which activates the cGAS-cGAMP-STING-mediated IFN response, demonstrated robust protection against HIV-1 challenge in vivo (26). Published evidence from vaccine and cancer studies also showed that cGAMP can induce potent B cell- and T cell-mediated adaptive immune response in mice (7, 10). Further experiments are needed to examine the efficacy of cGAMP-NP in protection against HIV-1 infection in humanized mice models.

We envision cGAMP-NP as a novel class of immune-stimulating ART that can be used for treating HIV as a long-acting agent. As more STING agonists and formulations enter clinical trials for antitumor therapy, we expect many of the concerns of adverse effects to be addressed, as well as more exciting opportunities for parallel development of these reagents for HIV therapy. Using cGAMP-NP or other STING agonists as adjuvants for HIV vaccines is another exciting possibility for future investigation.

## Acknowledgments

We thank Dr. Mamta Jain, Dr. Oladapo Abodunde, Minerva Santos, and Tianna Petersen at the University of Texas Southwestern Amelia Court HIV Clinic for patient recruitment, and members of the laboratories of N.Y., J.G., and Z.C. for helpful discussion.

## Disclosures

The authors have no financial conflicts of interest.

## References

1. Yan, N., and Z. J. Chen. 2012. Intrinsic antiviral immunity. *Nat. Immunol.* 13: 214–222.
2. Yan, N., A. D. Regalado-Magdos, B. Stigglebou, M. A. Lee-Kirsch, and J. Lieberman. 2010. The cytosolic exonuclease TREX1 inhibits the innate immune response to human immunodeficiency virus type 1. *Nat. Immunol.* 11: 1005–1013.
3. Gao, D., J. Wu, Y.-T. Wu, F. Du, C. Aroh, N. Yan, L. Sun, and Z. J. Chen. 2013. Cyclic GMP-AMP synthase is an innate immune sensor of HIV and other retroviruses. *Science* 341: 903–906.

4. Wheeler, L. A., R. T. Trifonova, V. Vrbanac, N. S. Barteneva, X. Liu, B. Bollman, L. Onofrey, S. Mulik, S. Ranjbar, A. D. Luster, A. M. Tager, and J. Lieberman. 2016. TREX1 knockdown induces an interferon response to HIV that delays viral infection in humanized mice. *Cell Rep.* 15: 1715–1727.

5. Hasan, M., and N. Yan. 2014. Safeguard against DNA sensing: the role of TREX1 in HIV-1 infection and autoimmune diseases. *Front. Microbiol.* 5: 193.

6. Chang, J. J., and M. Altfeld. 2010. Innate immune activation in primary HIV-1 infection. *J. Infect. Dis.* 202(Suppl. 2): S297–S301.

7. Li, X.-D., J. Wu, D. Gao, H. Wang, L. Sun, and Z. J. Chen. 2013. Pivotal roles of cGAS-cGAMP signaling in antiviral defense and immune adjuvant effects. *Science* 341: 1390–1394.

8. Parker, B. S., J. Rautela, and P. J. Hertzog. 2016. Antitumour actions of interferons: implications for cancer therapy. *Nat. Rev. Cancer* 16: 131–144.

9. Wang, H., S. Hu, X. Chen, H. Shi, C. Chen, L. Sun, and Z. J. Chen. 2017. cGAS is essential for the antitumor effect of immune checkpoint blockade. *Proc. Natl. Acad. Sci. USA* 114: 1637–1642.

10. Corrales, L., L. H. Glickman, S. M. McWhirter, D. B. Kanne, K. E. Sivick, G. E. Katibah, S.-R. Woo, E. Lemmens, T. Banda, J. J. Leong, et al. 2015. Direct activation of STING in the tumor microenvironment leads to potent and systemic tumor regression and immunity. *Cell Reports* 11: 1018–1030.

11. Li, L., Q. Yin, P. Kuss, Z. Maliga, J. L. Millán, H. Wu, and T. J. Mitchison. 2014. Hydrolysis of 2'3'-cGAMP by ENPP1 and design of nonhydrolyzable analogs. *Nat. Chem. Biol.* 10: 1043–1048.

12. Li, Y., T. Zhao, C. Wang, Z. Lin, G. Huang, B. D. Sumer, and J. Gao. 2016. Molecular basis of cooperativity in pH-triggered supramolecular self-assembly. *Nat. Commun.* 7: 13214.

13. Luo, M., H. Wang, Z. Wang, H. Cai, Z. Lu, Y. Li, M. Du, G. Huang, C. Wang, X. Chen, et al. 2017. A STING-activating nanovaccine for cancer immunotherapy. *Nat. Nanotechnol.* 12: 648–654.

14. Vermeire, J., E. Naessens, H. Vanderstraeten, A. Landi, V. Iannucci, A. Van Nuffel, T. Taghion, M. Pizzato, and B. Verhasselt. 2012. Quantification of reverse transcriptase activity by real-time PCR as a fast and accurate method for titration of HIV, lenti- and retroviral vectors. *PLoS One* 7: e50859.

15. Pizzato, M., O. Erlwein, D. Bonsall, S. Kaye, D. Muir, and M. O. McClure. 2009. A one-step SYBR Green I-based product-enhanced reverse transcriptase assay for the quantitation of retroviruses in cell culture supernatants. *J. Virol. Methods* 156: 1–7.

16. Wang, Z., M. Luo, C. Mao, Q. Wei, T. Zhao, Y. Li, G. Huang, and J. Gao. 2017. A redox-activatable fluorescent sensor for the high-throughput quantification of cytosolic delivery of macromolecules. *Angew. Chem. Int. Ed. Engl.* 56: 1319–1323.

17. Dobbs, N., N. Burnaevskiy, D. Chen, V. K. Gonugunta, N. M. Alto, and N. Yan. 2015. STING activation by translocation from the ER is associated with infection and autoinflammatory disease. *Cell Host Microbe* 18: 157–168.

18. Zhou, K., H. Liu, S. Zhang, X. Huang, Y. Wang, G. Huang, B. D. Sumer, and J. Gao. 2012. Multicolored pH-tunable and activatable fluorescence nanoplat-form responsive to physiologic pH stimuli. *J. Am. Chem. Soc.* 134: 7803–7811.

19. Zhang, X., H. Shi, J. Wu, X. Zhang, L. Sun, C. Chen, and Z. J. Chen. 2013. Cyclic GMP-AMP containing mixed phosphodiester linkages is an endogenous high-affinity ligand for STING. *Mol. Cell* 51: 226–235.

20. Landovitz, R. J., R. Kofron, and M. McCauley. 2016. The promise and pitfalls of long-acting injectable agents for HIV prevention. *Curr. Opin. HIV AIDS* 11: 122–128.

21. Woo, S.-R., L. Corrales, and T. F. Gajewski. 2015. Innate immune recognition of cancer. *Annu. Rev. Immunol.* 33: 445–474.

22. Fu, J., D. B. Kanne, M. Leong, L. H. Glickman, S. M. McWhirter, E. Lemmens, K. Mechette, J. J. Leong, P. Lauer, W. Liu, et al. 2015. STING agonist formulated cancer vaccines can cure established tumors resistant to PD-1 blockade. *Sci. Transl. Med.* 7: 283ra52.

23. Taylor, B. S., S. A. Olender, H.-V. Tieu, and T. J. Wilkin. 2016. CROI 2016: advances in antiretroviral therapy. *Top. Antivir. Med.* 24: 59–81.

24. Tsai, A., A. Irrinki, J. Kaur, T. Cihlar, G. Kukolj, D. D. Sloan, and J. P. Murry. 2017. Toll-like receptor 7 agonist GS-9620 induces HIV expression and HIV-specific immunity in cells from HIV-infected individuals on suppressive anti-retroviral therapy. *J. Virol.* 91: e02166–e16.

25. Offersen, R., S. K. Nissen, T. A. Rasmussen, L. Østergaard, P. W. Denton, O. S. Søgaard, and M. Tolstrup. 2016. A novel Toll-like receptor 9 agonist, MGN1703, enhances HIV-1 transcription and NK cell-mediated inhibition of HIV-1-infected autologous CD4+ T cells. *J. Virol.* 90: 4441–4453.

26. Wheeler, L. A., and J. Lieberman. 2014. Inhibiting the host exonuclease TREX1 induces a localized and protective host interferon response against acute HIV infection in vivo. *AIDS Res. Hum. Retroviruses* 30(Suppl. 1): A41.